



Distinguishing Late Holocene Storm Deposit From Shore-normal Beach Sediments From the Gulf of Thailand

Stapana Kongsen, Sumet Phantuwongraj* and Montri Choowong

Morphology of Earth Surface and Advanced Geohazards in Southeast Asia Research Unit (MESA RU), Department of Geology, Faculty of Science, Chulalongkorn University, Bangkok, Thailand

OPEN ACCESS

Edited by:

Basilios Tsikouras,
Universiti Brunei Darussalam, Brunei

Reviewed by:

Noureddine Elmejdoub,
Gabes University, Tunisia
Robert C Witter,
United States Geological Survey
(USGS), United States

*Correspondence:

Sumet Phantuwongraj
phantuwongraj.s@gmail.com

Specialty section:

This article was submitted to
Quaternary Science, Geomorphology
and Paleoenvironment,
a section of the journal
Frontiers in Earth Science

Received: 04 November 2020

Accepted: 11 January 2021

Published: 22 February 2021

Citation:

Kongsen S, Phantuwongraj S and
Choowong M (2021) Distinguishing
Late Holocene Storm Deposit From
Shore-normal Beach Sediments From
the Gulf of Thailand.
Front. Earth Sci. 9:625926.
doi: 10.3389/feart.2021.625926

Grain size, as one of sedimentological proxies, coupled with a detailed description of the sedimentary structures and luminescence dating were used to unveil the sediment sources and transport process of the Holocene ancient coastal storm events recorded in the beach ridge plain, wet swale and muddy environments at Prachuap Khiri Khan, in the Southern Peninsula of Thailand. In this study, a total of 141 sand samples were collected from the shore-normal ridge-swale topography and analyzed for layers of candidate storm deposits, revealing at least 21 candidate coastal storm events. The grain size distribution of beach sediments was, in general, unimodal, while the candidate storm sediments revealed a mixed combination of multimodal, bimodal and unimodal distributions. Plots of mean grain size against skewness and kurtosis and of skewness against kurtosis could differentiate storm deposits from shore-normal beach sediments. Sedimentary structures preserved in the ancient coastal storm deposits included parallel and inclined landward laminations, mud rip-up clasts, layers of shell fragments, a pebble grain, normal and reverse grading and sharp lower and upper contacts. Candidate storm layers overlain on a dry beach ridge intervened with mud in a swale showed a finer and thinner landward deposit. Marine shell fragments, smaller foraminifers, ostracod and scaphopod (tusk shell), were well preserved. Based on optically stimulated luminescence dating and a correlated accelerator mass spectrometry age, multiple layers of sand derived from different frequencies of coastal storms were deposited over the middle to late Holocene.

Keywords: storm deposit, holocene, southern peninsular Thailand, grain size analysis, luminescence dating

INTRODUCTION

Along the world's coastlines, it is necessary for coastal communities to prepare for the inevitable effects of extreme coastal disasters, such as typhoons or hurricanes, which are one of the direct results from the present day global climate variations. The appropriate coastal management, defensive measure, warning system and emergency evacuation procedure to mitigate from these extreme events should be taken into account seriously. At present, the sedimentary record is one of the geological evidences that can be used to indicate previous environmental changes and the coastal mechanism of high energy events, such as tsunamis and extreme coastal storms. High energy events that cause an abrupt flooding of sea water can form deposits of sand layers inland (commonly known as washover deposits) that vary in shape, thickness and the preservation potential of sedimentary structures (Donnelly, 2005). The existence of washover deposits on both the surface and subsurface is

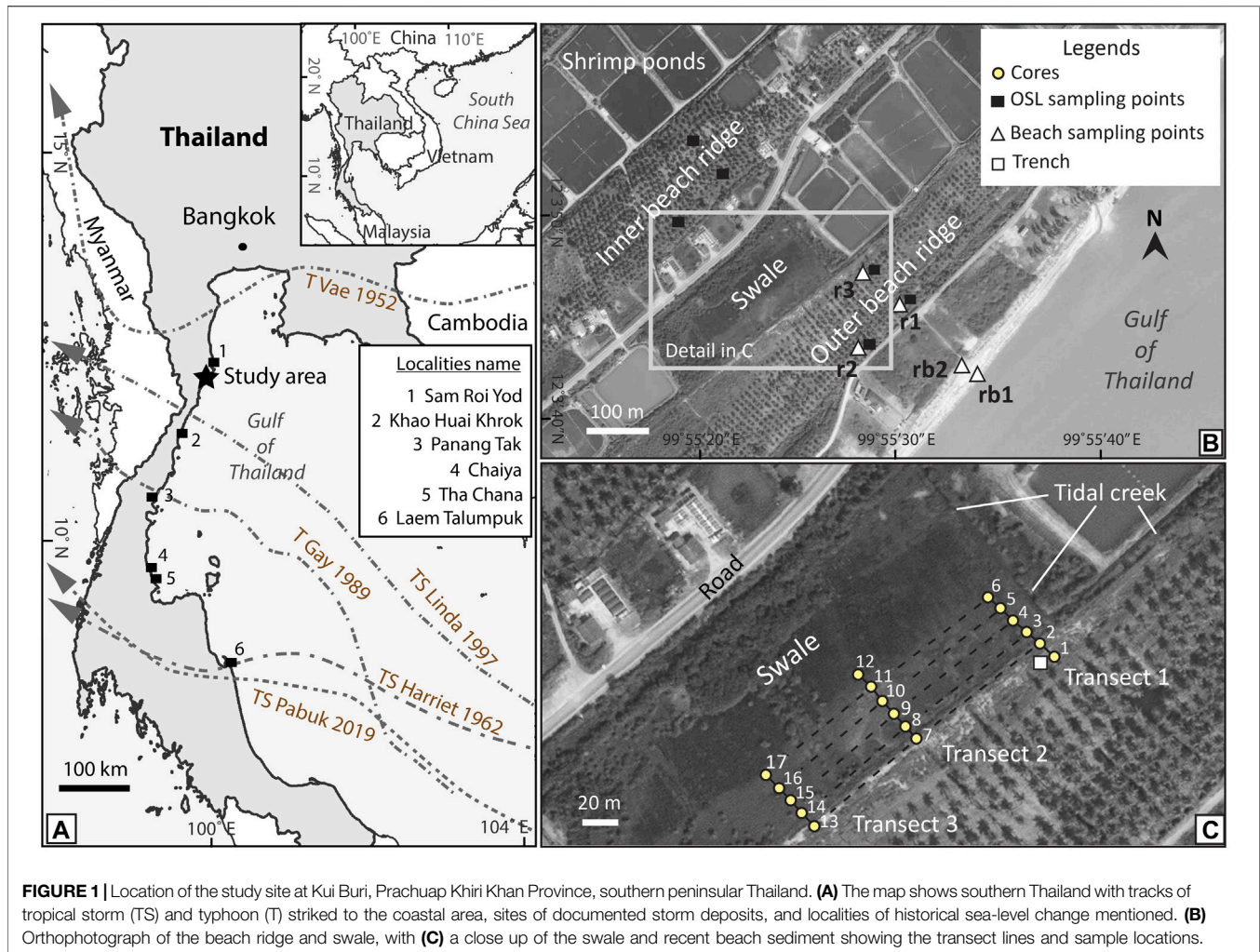


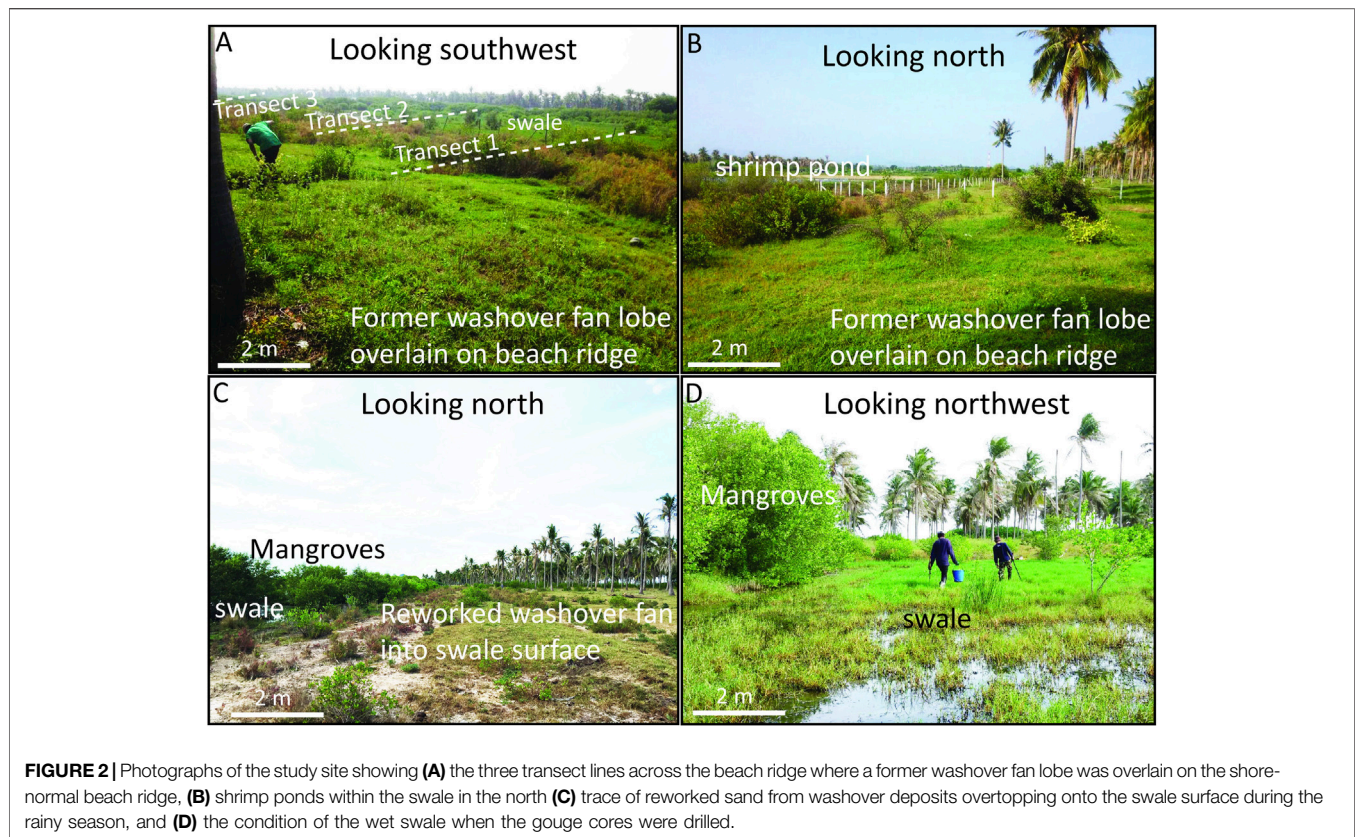
FIGURE 1 | Location of the study site at Kui Buri, Prachuap Khiri Khan Province, southern peninsular Thailand. **(A)** The map shows southern Thailand with tracks of tropical storm (TS) and typhoon (T) striked to the coastal area, sites of documented storm deposits, and localities of historical sea-level change mentioned. **(B)** Orthophotograph of the beach ridge and swale, with **(C)** a close up of the swale and recent beach sediment showing the transect lines and sample locations.

evidence to support that the area had been affected by coastal storm events. Therefore, searching for geological records of coastal storms in the past is important for building future communities with coastal resilience.

In Thailand, candidate sand sheets of extreme coastal storm events have been recognized (e.g., Phantuwoongraj et al., 2008; Phantuwoongraj et al., 2010; Phantuwoongraj and Choowong, 2012; Kongsen et al., 2016; Williams et al., 2016). The characteristics and sedimentary structures of a storm overwash deposit include lamination, normal and reverse grading, washover fan, mud rip-up clast, sharp top and basal contacts, wedge shape, marine shell assemblage, marine microfossils, and diatoms (e.g., Liu and Fearn, 1993; Liu and Fearn, 2000a; Liu and Fearn, 2000b; Donnelly et al., 2001; Liu, 2004; Donnelly, 2005; Elsner, 2007; Liu, 2007; Williams, 2010; Phantuwoongraj et al., 2013; Williams, 2013; Williams et al., 2016). Furthermore, they are often identified in paleotempestological studies. Paleotempestology investigates buried offshore and/or beach sediments that were transported inland by prehistorical storm surge waves on low-lying areas that are located abruptly behind the sea and then

preserved well by muddy sedimentation in the low energy condition. These form a sand layer that is a key indicator of a coastal storm event archived in the geological record (Liu and Fearn, 1993; Liu and Fearn, 2000a; Liu and Fearn, 2000b; Liu, 2004; Liu, 2007).

However, recognizing an anomalous sand layer buried in the subsurface of various coastal environments from an extreme coastal disaster (high energy event) has a number of difficulties. A way to distinguish coastal storm and tsunami deposits is still needed, although various diagnostic keys to define these events have been reported and developed (e.g., Nanayama et al., 2000; Goff et al., 2004; Tuttle et al., 2004; Kortekaas and Dawson., 2007; Morton et al., 2007; Nott, 2007; Choowong et al., 2008; Jankaew et al., 2008; Komatsubara et al., 2008; Phantuwoongraj and Choowong, 2012). The depositional process of these events depends on several controlling factors from place to place, such as the intensity of the event, duration, surge height, types of vegetation, beach morphology, elevation, micro-topography, sediment supply, sediment composition, and mineralogy (Morton and



Sallenger, 2003; Tuttle et al., 2004; Jagodziński et al., 2012; Phantuwongraj and Choowong, 2012).

It is known that Thailand has been exposed to five extreme coastal storms (two typhoons and three tropical storms) in the past century. These were the typhoon Vae (1952), tropical storm Harriet (1962), typhoon Gay (1989), tropical storm Linda (1997), and tropical storm Pabuk (2019) (Figure 1A). Typhoon Gay in 1989 was considered as one of the worst case extreme coastal storm events in the Gulf of Thailand (GOT) and led to catastrophic damages to the country with a cost of at least 11 billion Bahts and about 800 fatalities (Vongvisessomjai, 2009; Williams et al., 2016). However, Thailand only started keeping official records of storm data from 1951, and so the prehistoric and historic records are lacking.

Consequently, with several attempts to improve our understanding regarding geological records of historic and prehistoric coastal storm events in Thailand, the major objectives of this paper were aimed to 1) present a sedimentological approach for discriminating storm and beach deposits based on sedimentary criteria; and 2) to use of statistical grain size parameters derived from grain size analysis as a locally valid indicator for sediment source and the transport process found from ancient coastal storm deposits. In addition, this study also expands the sedimentological work of Williams et al. (2016) regarding regional cyclone frequency based on the optically stimulated luminescence (OSL) dating and a correlated age that provides chronological representative ages of an event.

GEOLOGICAL SETTING OF THE STUDY AREA

Kui Buri Area

We continued and extended the search for possible ancient storm deposits in the same swale but further to the north 2 km where Williams et al. (2016) discovered them from Kui Buri, Prachuap Khiri Khan Province, southern peninsular, Thailand. The hypothesis was that the distinctive features of the geomorphological setting here was the potential preservation site of prehistoric coastal storm events. Particularly, the low-lying swale behind the beach ridge was the targeted area (Figure 1B). This swale is located at $12^{\circ} 03' 46''$ N and $99^{\circ} 55' 24''$ E between two beach ridges that we named as the outer and inner beach ridge (Figure 1B). The outer beach ridge was located 450 m perpendicular and 300 m long parallel to shoreline. Three transect lines were measured (Figure 2A). Although, parts of the swale in the north and south of the study area have been modified by the construction of shrimp ponds (Figure 2B), the selected study area has not been disturbed by anthropogenic activity (Kongsen et al., 2016).

The floor of the swale is 0.6 m above mean tide level (MTL). Fine-grained particles (silt and clay) were found on the subaqueous ground surface of the swale, which presumably were transported during heavy rainfall and/or flooding from a tidal channel during high tides (Figure 2C). Thus, the sedimentation of swale environment here is likely to be

relatively constant and from a low energy condition. The water level in the swale varies from 10 to 50 cm depth, depending on the local swale topography (**Figure 2D**). Also, tidal creeks, sedge and mangrove (*Rhizophora apiculata*) were commonly observed. During site reconnaissance, sand compounded with broken shell debris was observed, and was on the back part of the outer beach ridge surface which was possibly transported from beach and offshore area.

Additionally, the habitat of marine species, especially recent foraminifera has been investigated in the GOT where is located closed to this study area. Jumnonngthai. (1983) collected the sediment samples of sand surface (station 1) in the GOT in order to study recent foraminifera at 36 m depth from the sea surface. 16 genera of benthic foraminifers and ostracods were found which consisted of *Ammonia* sp., *Amphistegina* sp., *Asterorotalia pulchella*, *Cellanthus craticulatus*, *Cibicides* spp., *C. wuellerstorfi*, *Elphidium* spp., *Florilus* sp., *Miliammina* sp., *Operculina ammonoides*, *Quinqueloculina* spp., *Reophax* spp., *Reusella* sp., *Rotalia* spp. and *Textularia* sp. Most of them are common in the shallow water which live between depths of 29–74 m.

According to the literatures of the history of sea-level highstand and beach ridge progradation, the age of sea notch at Sam Roi Yod National Park, near the study area (**Figure 1A**), and beach ridge plain at Kui Buri, Prachuap Khiri Khan has been reported (Choowong et al., 2004; Surakiatchai et al., 2018). The age of ¹⁴C radiocarbon dating from oysters at the sea notch walls at Sam Roi Yod National Park provided the period of time the oysters lived in and tentatively reflected two breaks in the gradual regression, times when the sea level had been stable which linked to the sea level high stand around 6,500 years ago (Surakiatchai et al., 2018). The highstand was at 3–4 m height above the present MSL, as evidenced from the small uppermost sea notch. The OSL dating data of beach ridge plain at Kui Buri also revealed the progradation of beach ridge started after the sea level reached the highstand at around 7,000 years ago (Surakiatchai et al., 2018). The beach ridge and swale in this research (inner and outer beach ridge) (**Figure 1B**) locate at the outermost part of beach ridge series resulted from the period of sea level regression (Choowong et al., 2004; Surakiatchai et al., 2018).

Impact of Past Coastal Storms

With respect to the impact from modern coastal storm events, when considering the storm tracks (**Figure 1A**), it seems that the sedimentary traces of these coastal storms would be preserved in the area where the coastal storms approached or traversed across. However, sedimentary analysis of these modern coastal storms in this site has not been performed. Rather, reports on coastal storm deposits and paleotempestology research in Thailand are sparse. Roy (1990) reported the remains of sedimentary clues from typhoon Gay, which hit Thailand in December 1989, at a small beach in the GOT at the Khao Huai Khrok area (**Figure 1A**), Prachuap Khiri Khan, southern peninsular, where 40 cm thick sand mixed with heavy minerals was found. Floating debris (storm marker) was observed at an elevation around 1.6 m above high tide level.

Almost 2 decades later, Phantuwongraj et al. (2008) described sand sheets, varying from 4 to 60 cm in thickness, found in a muddy environment near Chaiya, Tha Chana and Leam Talumpuk (**Figure 1A**), southern peninsular in the GOT. The detailed sedimentary structures described by Phantuwongraj et al. (2008) contained sharp upper and lower contacts with the muddy layers, and they suggested these unusual sand layers were likely to be potential sedimentary traces of tropical storm Harriet (1962), typhoon Gay (1989) and tropical storm Linda (1997).

Subsequently, Phantuwongraj et al. (2010) described multiple layers of paleo-storm sand sheets found in a swale located 1 km inland from the present shoreline near Panang Tak area (**Figure 1A**), Chumphon, southern peninsular, in the GOT. However, in both these places, the depositional ages of the candidate storm sand sheets have not been confirmed since no dating data was available (Phantuwongraj et al., 2008; Phantuwongraj et al., 2010).

Similarly, tropical storm Linda hit the Kui Buri area in 1997 and was not only comprised of a landfall close to this study area, but its track way also ran across the Prachuap Khiri Khan area to the west coast at the Andaman Sea (**Figure 1A**). However, no reported sedimentary traces of tropical storm Linda have been found. Therefore, we infer that the missing sediments of tropical storm Linda may be caused either by the disturbance from anthropogenic activity along the coastal area, such as recreational construction (resorts and hotel), fisheries (shrimp and fish pond farming) and coastal agriculture, or the spontaneous reworking and erosional processes.

APPROACH AND METHODS

Remotely Sensed Data Interpretation and Topographic Survey

Aerial photographs and satellite images of Kui Buri area were interpreted to locate swales or lowlands most likely to preserve ancient storm deposits. To confirm the interpretation of the data from aerial photographs and satellite images, field checks were performed after finishing the coastal geomorphologic interpretation.

Beach profiles (**Figure 3A**) were surveyed using a total station survey camera SOKKIA (SET630R), where surveying was performed at sea level and measured westwards across the outer beach ridge, swale and inner beach ridge respectively (**Figures 3A,B**). Distance measurement using the fine average measurement mode with prism, which the accuracy is $\pm (2 + 2 \text{ ppm} \times D)$ mm. All stations were also referenced by a hand-held GPS. Moreover, topographic profiles were referenced to local tide level at the time of survey. Then, elevation were converted to meters a.m.s.l. by following the method of Williams et al. (2016) using tide tables obtained from the nearest tide gauge stations at Ko Lak, about 25 km south of Kui Buri (Thai Royal Navy, 2015). At Kui Buri, mean sea level is 1.61 m above the tide datum of mean lowest low water (m.l.l.w.) and MTL range was 1.05 m. The MTL was set to zero point, whereas the high tide level HTL and low tide level LTL ranged 0.525 m from the top and the bottom lines of the zero point (**Figure 3**).

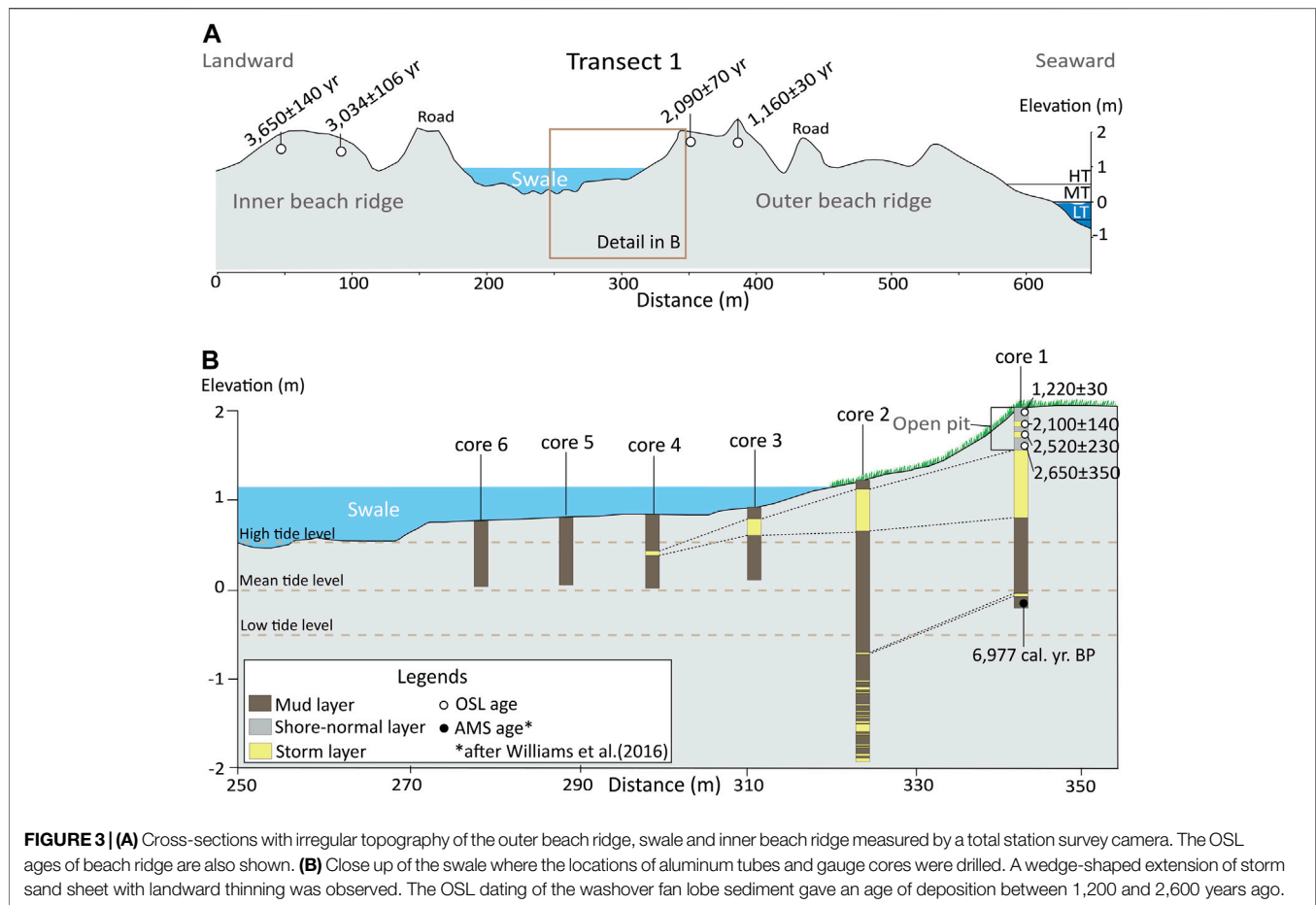


FIGURE 3 | (A) Cross-sections with irregular topography of the outer beach ridge, swale and inner beach ridge measured by a total station survey camera. The OSL ages of beach ridge are also shown. **(B)** Close up of the swale where the locations of aluminum tubes and gauge cores were drilled. A wedge-shaped extension of storm sand sheet with landward thinning was observed. The OSL dating of the washover fan lobe sediment gave an age of deposition between 1,200 and 2,600 years ago.

Sediment Sampling and OSL Dating

Site reconnaissance was conducted by a gouge core to estimate the depth of the potential ancient storm layer under the subsurface at around 2 m depth. After examining subsurface sediments and finding anomalous sand layers, coring was applied to retrieve the stratigraphy along three transects in the swale perpendicular to the shoreline at a distance from 350 to 450 m inland (**Figure 1C**). An aluminum tube of 3 inch in diameter and 2 mm thick was used and a total of 17 core samples were dug (cores 1–17). All cores were of 1–3 m depth from the surface. All coring locations were referenced by a hand-held GPS. The space between each core was about 7–8 m.

All sample cores retrieved from the swale were sealed by duct tape and then transported to the sedimentology lab at the Department of Geology, Faculty of Science, Chulalongkorn University for analyzing and sampling. Aluminum cores were cut lengthwise and sediment samples within cores were divided into two sides crosswise. Then, logging and photographing of each core was performed. Nearly all the retrieved core samples showed a continuity in the candidate storm-induced washover deposits, the exceptions being some cores in the central swale (cores 5, 6, 11, 12, 16, and 17; **Figure 1C**). However, core samples of transect 1 are solely described in this paper because the rest of cores yielded similar characteristics as candidate washover deposits.

In transect 1, candidate storm layers were only recognized in cores 1–4. Samples of the candidate storm sediment were then picked at every 0.5 cm, especially in the place where sedimentary structures (lamination) were observed. Unstructured candidate storm layers were collected every 1 cm. For comparative analysis, beach sediments that originated from the shore-normal process were collected, and are named here as recent beach 1, recent beach 2, and ridge sediments 1–3 (**Figure 1B**).

A total of 136 samples picked up from candidate layers of ancient storm and five samples of beach sediments were analyzed using the laser granulometric method, and the data were computed using the logarithmic method of moments (Krumbein and Pettijohn, 1938; McBride, 1971; Blott and Pye, 2001). In addition to grain size analysis, all selected sediments were discriminated into sub-samples to detect their physical properties, including composition (Fritz and Moore, 1988; Rothwell, 1989; Rosenthal et al., 2018), roundness and sphericity (Powers, 1953), under a light microscope. Sub-samples were first dried in an oven at 70°C for 24 h, and then dry-sieved through a 63 μm sieve (mesh 230) to gain a sand fraction without finer particles. By doing this, a clear visualization of the sand assemblages under a microscope for identifying each mineral could be conducted without the problem of the finer-grains surrounding the sample and masking the view.

TABLE 1 | Results of OSL dating from inner, outer beach ridges and trench.

Sample	Depth (cm)	U (ppm)	Th (ppm)	K (%)	Water (%)	AD (Gy/ka)	ED (Gy)	Age (yr)
K1	40	0.78 ± 0.01	2.04 ± 0.01	0.37 ± 0.002	2.48	0.614 ± 0.01	0.718 ± 0.01	1,160 ± 30
K2	40	0.53 ± 0.01	1.92 ± 0.01	0.31 ± 0.002	1.37	0.517 ± 0.01	1.083 ± 0.03	2,090 ± 70
K3	40	0.69 ± 0.01	2.26 ± 0.01	0.36 ± 0.002	2.44	0.605 ± 0.01	0.744 ± 0.02	1,220 ± 40
K4	40	0.68 ± 0.01	1.87 ± 0.01	0.26 ± 0.002	2.26	0.497 ± 0.01	1.51 ± 0.28	3,034 ± 106
K5	40	0.49 ± 0.01	1.53 ± 0.01	0.32 ± 0.002	1.81	0.481 ± 0.01	1.758 ± 0.05	3,650 ± 140
K6	40	0.66 ± 0.01	2.28 ± 0.01	0.32 ± 0.002	1.76	0.743 ± 0.01	1.832 ± 0.01	3,190 ± 100
K7	20	0.73 ± 0.01	3.38 ± 0.01	0.77 ± 0.002	6.89	0.970 ± 0.01	1.186 ± 0.04	1,220 ± 30
K8*	50	0.71 ± 0.01	0.45 ± 0.01	0.84 ± 0.002	29.74	0.738 ± 0.01	1.55 ± 0.1	2,100 ± 140
K9*	65	1.01 ± 0.01	4.74 ± 0.01	0.93 ± 0.002	23.40	0.993 ± 0.01	2.51 ± 0.23	2,520 ± 230
K10	85	1.10 ± 0.01	5.52 ± 0.01	1.09 ± 0.002	25.82	1.106 ± 0.01	2.931 ± 0.39	2,650 ± 350

*The results of OSL dating at the candidate storm layers.

AD = Annual Dose, ED = Equivalent dose. All ages are quoted in years before A.D. 1950.

Furthermore, in the fieldwork along the outer and inner beach ridges, we excavated small pits at approximately 40 cm depth from the beach ridge surface for collecting quartz-rich materials to be used for the OSL dating. A total of six OSL samples were collected for establishing the lateral age of the beach ridge formation. The locations of the OSL sample sites are shown in **Figure 1B**. In addition, a further four OSL samples were collected at the back of the outer beach ridge vertically. A trench of 85 cm depth was dug here and the deeper samples were made by coring (core 1). The trench profile itself contained two candidate storm layers at 50–58 cm and 65–72 cm depth intercalated with shore-normal beach ridge deposits (**Figure 3**). Distinguishing storm and beach deposits from sand-over-sand features in a trench is always challenging. In principle, we differentiated them using the difference in color of the sand layers and the presence of marine shell fragments as a key to define candidate storm layers in the field. A number of marine micro-organisms, including foraminifera, ostracods and scaphopods (tusk shell), were found in the candidate storm sediments, while almost 99% of quartz is the main composition of shore-normal layers.

All locations of OSL samples were referenced by a hand-held GPS. A total of 10 OSL samples, designated as K1 to K10 (**Table 1** and **Figure 1**), were obtained and then divided into two parts for the equivalent dose (ED) and annual dose (AD) analysis. The ED samples collected from an approximately 40 cm depth from the ground surface were put in a 0.5 cm thick wall and 1.5 inches diameter of PVC tubes in order to avoid exposure to sunlight. Sand surrounding the ED samples were collected for AD analysis in a lightproof plastic bag. The OSL samples were analyzed by the Quaternary Dating Laboratory, Department of Geology, Faculty of Science, Chulalongkorn University, Bangkok, Thailand. A small portion of each AD sample was separated for water content analysis. The remains were dried at 40°C and sieved through an 841 µm (mesh 20) sieve and a pan. The pan sand fraction (290 g) was kept for measuring the natural radioisotopes concentration, including uranium (ppm), thorium (ppm) and potassium (%) using high-resolution gamma spectrometry, and analysis of the data was based on a standard table (Bell, 1979) and the calculated cosmic ray dose rate (Prescott and Hutton, 1994).

The ED samples were analyzed at night under a subdued red light. Samples of ED sands were wet-sieved through 74 and

250 µm sieves (mesh 60 and 200), and the 74–250 µm diameter sand fraction was etched by 25% (v/v) hydrofluoric acid for 20 min, washed with distilled water, cleaned with 35% (v/v) hydrochloric acid for 20 min, rinsed with distilled water and dried at 40°C for 48 h to obtain the purified quartz. The ferrominerals in the dried-aliquot-sized samples (74–250 µm) were then separated using an iso-dynamic magnetic separator to provide a homogeneity of the ED samples.

The OSL analysis of the ED samples was performed using a Risø OSL/TL reader equipped with a calibrated 90Sr/90Y beta radiation source and a blue (470 ± 20 nm) light source (Bøtter-Jensen, 1997; Bøtter-Jensen et al., 2000). Aliquot-sized grains were attached to a 9.8 mm diameter stainless-steel disc in a monolayer using silicone oil. The single-aliquot regenerative (SAR) technique was employed to assess all ED samples with test doses around 10% of the estimated natural dose (N) (Murray et al., 1987; Murray and Wintle, 2000). Based on the ED distribution, the minimum age model was applied in this study (Duller, 2008). The key criteria applied for rejection of individual ED value included recuperation <5%, the recycling ratio within 10%, test dose error <10%, depletion ratio within 10% of unity, adequate fit of the growth curve and enclosure of DE by regenerative doses. The OSL decay curve, growth curve, dose recovery, recycling ratio, and recuperation of each ED sample and each age are presented in an online **Supplementary Material**.

RESULTS

Stratigraphy and Sedimentary Structures From Core Samples

Core 1 (140 cm long) was located at 275 m from the present shoreline in the most seaward location of transect 1, and at a similar location of the trench (**Figure 3B**). The trench profile at 0–85 cm depth contained two candidate storm layers. We started collecting core 1 at the bottom surface of a trench (at 85 cm depth). Two additional candidate storm layers were found at 10–36 cm and 127–128.5 cm depth (**Figure 4**). At 36–127 cm depth, an oxidized mud layer was observed. Thus, we also collected four candidate storm layers found at the trench and

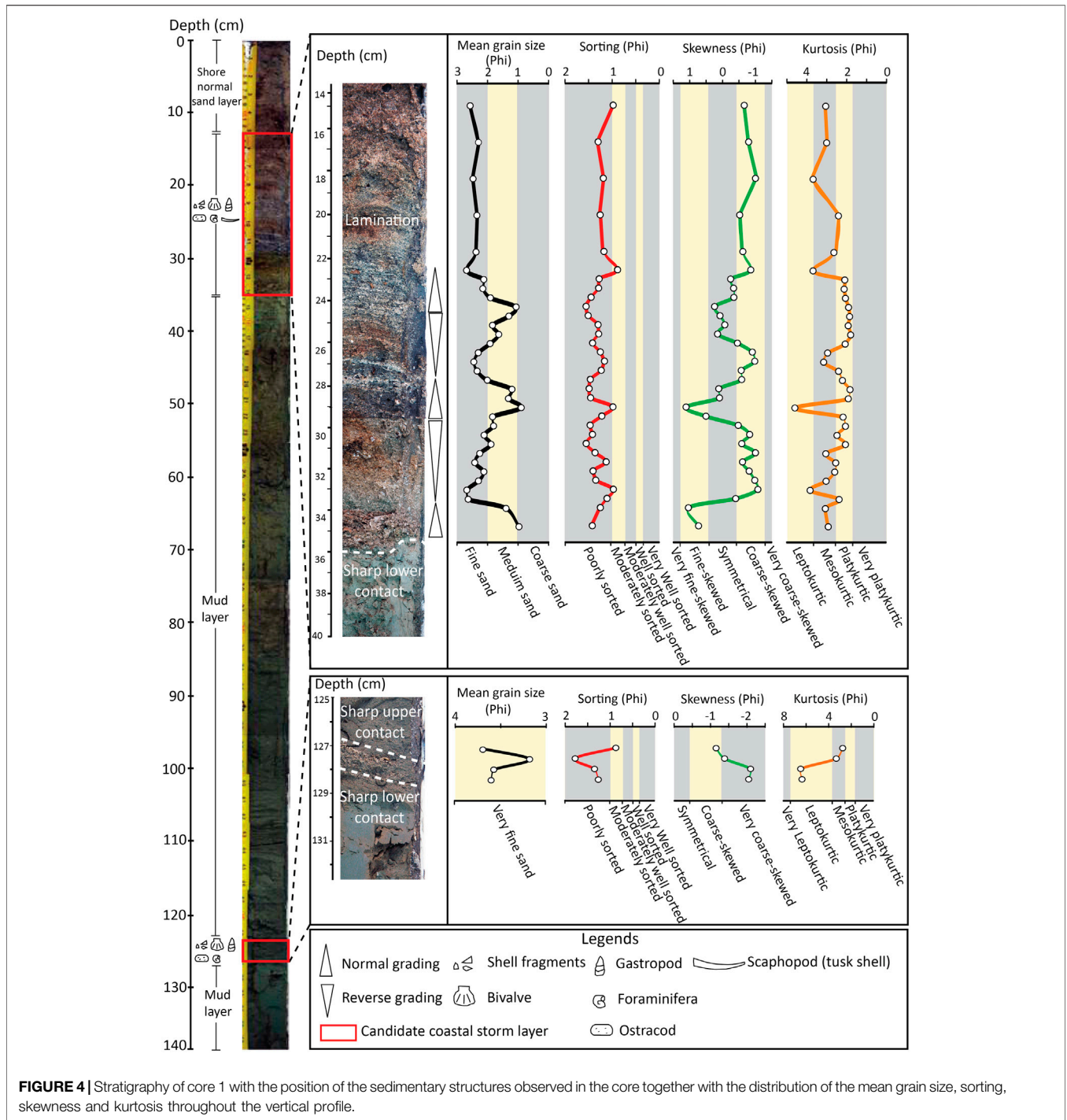
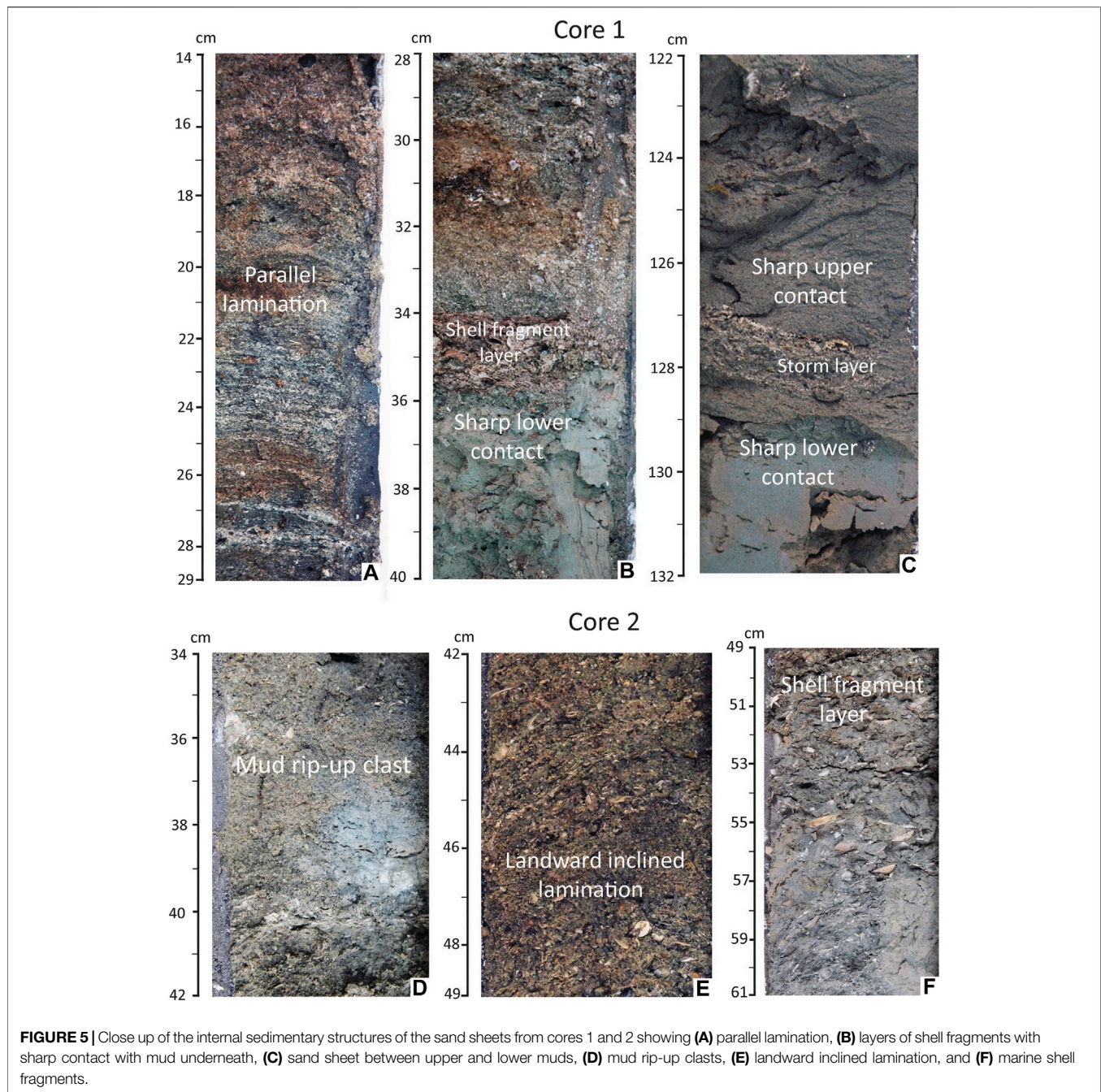


FIGURE 4 | Stratigraphy of core 1 with the position of the sedimentary structures observed in the core together with the distribution of the mean grain size, sorting, skewness and kurtosis throughout the vertical profile.

core 1, as appeared in the stratigraphy (Figure 3B). Sedimentary structures of these candidate storm layers in this core consisted of parallel lamination (Figure 5A), shell fragment layer (Figure 5B), sharp lower and upper contacts with mud layers (Figure 5C).

Core 2 was the longest core in transect 1 (300 cm long), and was located 7 m inland from core 1 (Figure 1C). Remarkably, a total of 21 candidate storm layers were recognized in this core. The first candidate storm was found at 20–55 cm depth,

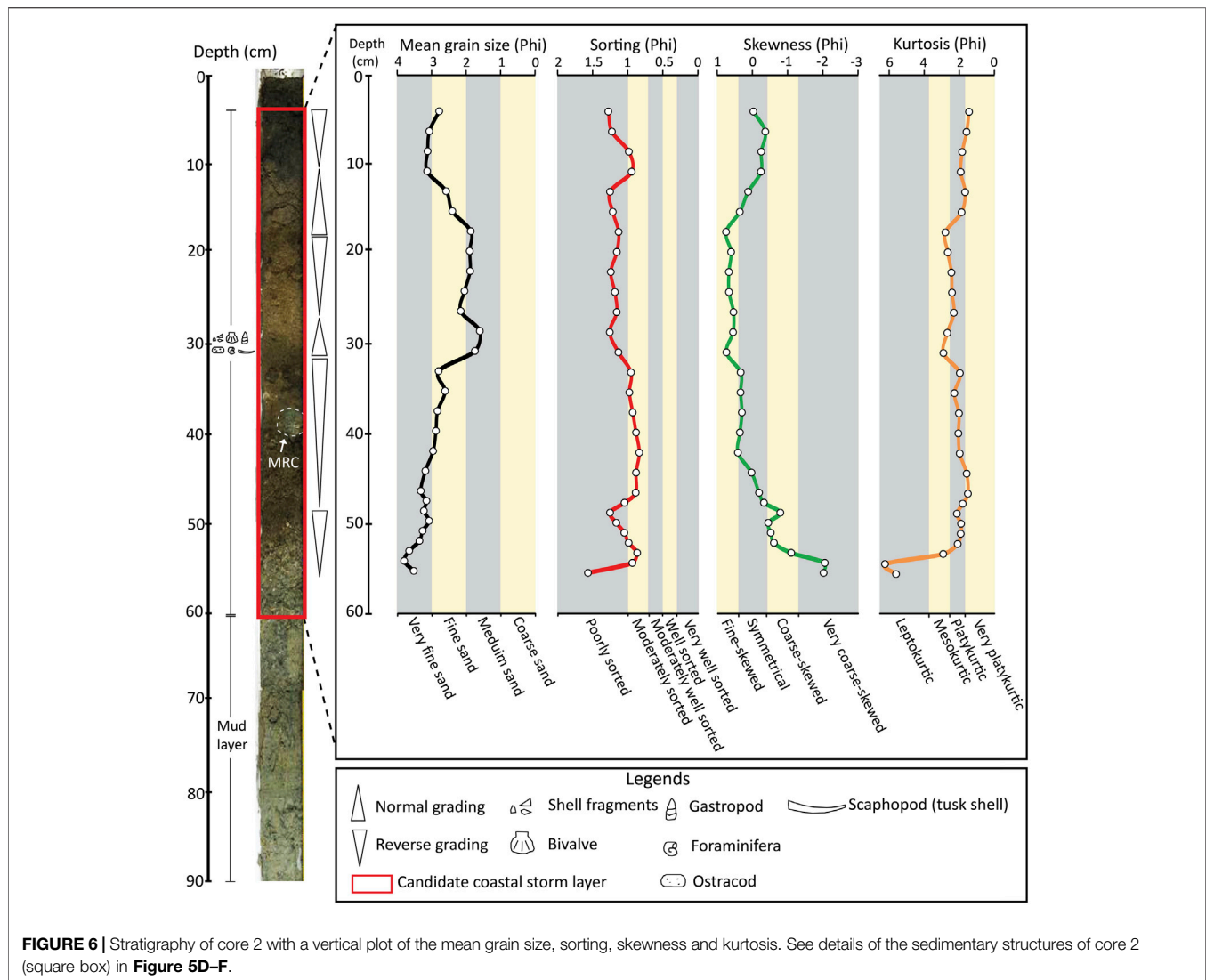
containing a gradational upper contact with black silty sand layer and a sharp basal contact with oxidized mud layer (Figure 6). Pebble and shell fragments were also observed in this candidate storm event. At 55–180 cm depth was a layer of oxidized mud deposits that likely belonged to the sediment of the swale environment. Below 180 cm depth, 20 dark gray layers of candidate storm events compounded with shell fragments were observed throughout the depth from 180 to 300 cm, each



interbedded with a dark mud layer, showing sharp top and lower contacts (Figures 3B, 8). Sedimentary structures of candidate storm layers in this core were mostly similar to the candidate layer of storm in core 1, especially the sharp upper and lower contacts. Remarkable sedimentary structures in this core included mud rip-up clasts (Figure 5D), inclined landward laminated sand (Figure 5E), and a shell fragment layer (Figure 5F). The inclined landward lamination observed in core 2 may represent the distal part of storm deposits (Figure 3B), where the flow contributed to the characteristic foreset bedding (Phantuwongraj et al., 2013).

Core 3 (80 cm long) was collected in the wet swale, and was located 7 m inland from core 2. One candidate storm layer compounded with shell fragments was found at 10–29 cm depth (Figure 7). Sedimentary structures contained sharp upper and lower contacts with oxidized mud layers. Notably, a pebble was also observed at 28 cm depth. Bioturbation, such as rootlets, appeared on the top of core.

Core 4 was 80 cm long and was collected in similar wet swale to Core 3. One thin layer of an inclined landward candidate storm sand compounded with shell fragments was observed at 41–45 cm depth. This candidate storm layer showed sharp



upper and lower contacts with oxidized mud layers. Cores 5 and 6, 62 and 67 cm long, respectively, were collected in a similar wet swale to Cores 3 and 4. The candidate storm sand layer was absent, but an oxidized mud layer was observed in both cores. The absence of the candidate storm sand layer in these cores may be associated with the low intensity of the storm surge energy.

At transect 1, based on the thickness of the candidate coastal storm layers that appeared in the stratigraphy of cores 1–4, the first candidate storm layers of each core were correlated using the sharp contacts, color of sand layer, composition, marine fossil and microfossil. The characteristic of thinner landward deposits or a wedge-like shape was clearly observed (**Figure 3B**).

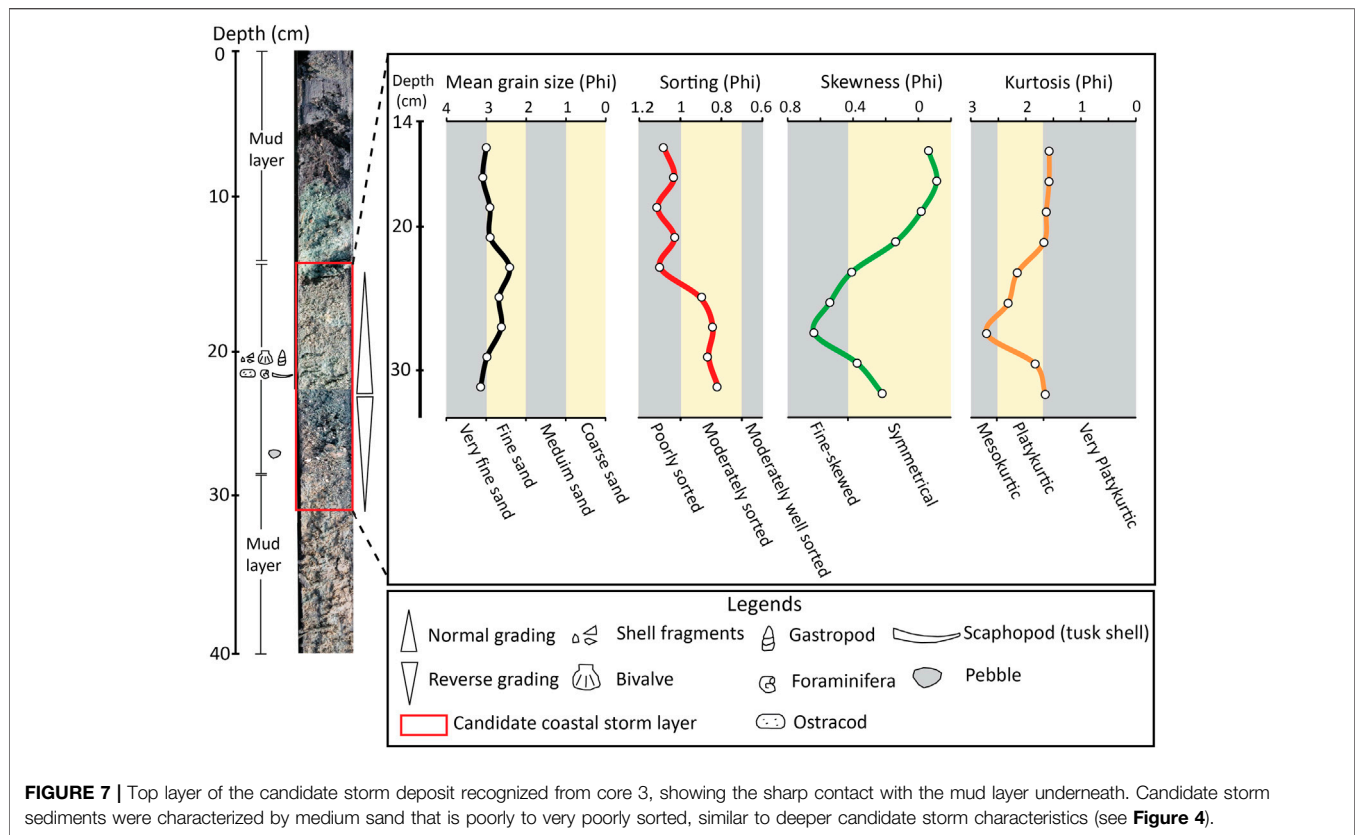
Additionally, the longest cores from transects 1–3 (Cores 2, 7 and 13) were collected parallel to beach orientation and the correlation is shown in **Figure 8**. Storm unit 1 is thickest and located in a distal part of a washover fan lobe. As mentioned above, the major keys used to correlate the candidate storm layer include the existence of marine fauna and microfauna, sharp contact, color of sand layer, thickness, and composition.

However, the number of depositional events in the candidate storm layers found in each core differed. The maximum and minimum number of candidate coastal storm layers, 21 and 12 layers, were recognized at cores 2 and 7, respectively. Core 13 was composed of 13 candidate storm layers.

Sedimentological Properties of Sand Sheets

Composition

Sediment composition of the candidate storm and the recent beach 1 and 2 (presented in an online **Supplementary Material**) consisted mostly of quartz, feldspar, heavy mineral, shell fragment debris, marine shell fossils (bivalves and gastropods) and marine microorganisms (foraminifera, ostracods and scaphopods) (see location of sampling points in **Figure 1B**). Sand sediments from beach ridge samples 1–3 contained almost totally quartz sand without bioclast. The sediment composition of recent beach 1 and 2 was relatively similar to the candidate storm sediments



found in the swale environment, which varied between 60 and 70% quartz sand and 20–30% bioclast. The rest of composition was feldspar and heavy minerals in a very low content (1–3%). However, there were some samples of candidate storm sediment that contained a high percentage of bioclast content of up to 70%. The increased bioclast content from top to bottom at depths of 21–36 cm in core 1 was dominant. Marine microfossils, especially foraminifera, ostracod and scaphopod (tusk shell), were found dominantly in all candidate storm sediment samples.

The variety of sphericity and roundness of the sand found in the candidate storm sediments (presented in an online **Supplementary Material**) varied from low to high with very angular to sub-rounded sand. On the other hand, beach sediments usually showed a high sphericity with sub-angular to sub-rounded sand, except for the sediment of ridge 3 that was classified as very angular to sub-angular with a low sphericity. It is suggested that in general that the grain properties and types of marine species were similar, due to remobilization of sediment in each coastal environmental zone to deposit in the swale by storm surges.

Grain Size and Grading

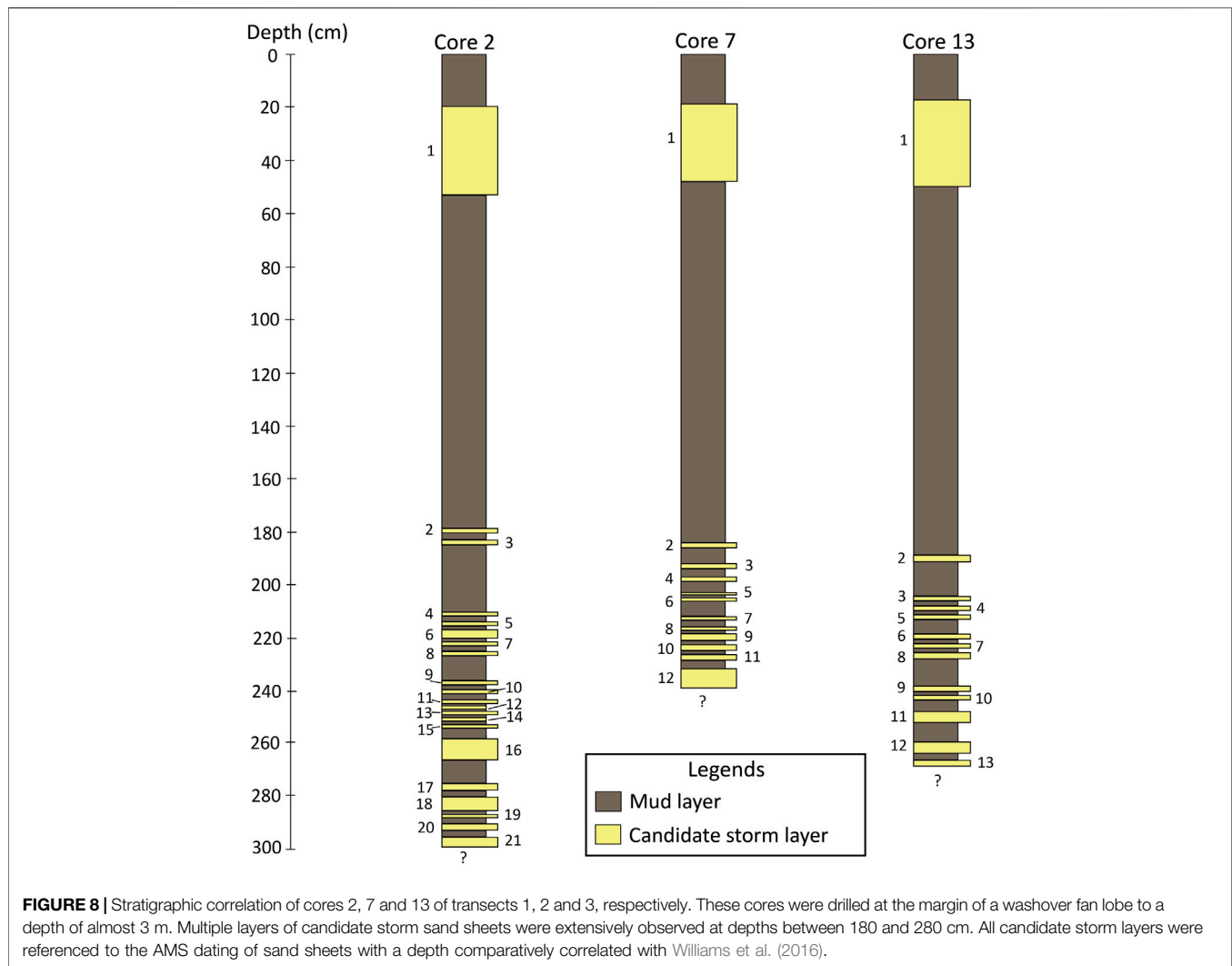
In this study, the mean grain size of the storm vs. the beach sediments was remarkably different. The mean grain sizes of sediment from recent beaches 1 and 2 and the inner beach ridge 3 were classified as fine sand varying between 2.33 and 2.41 phi scale, while ridge sediments 1 and 2 appeared as medium sand, ranging between 1.90 and 1.50 phi scale. Mean grain sizes of candidate storm

sand varied over a wide value, ranging from very fine to coarse sand (3.99–0.98 phi scale) but without very coarse sand. In addition, the mean grain sizes of the candidate storm sediments showed a clear vertical variation in core 1 (**Figure 4**). Three sets of normal and two sets of reverse grading were found within the laminated sand layer of core 1 (top to bottom). Grading of cores 1 and 2 showed several intervals of inverse and normal grading, whereas, core 3 showed only one part of inverse and normal grading.

The mean grain size of the candidate storm sediments of core 2 consisted mainly of very fine to fine sand. There were at least five samples that showed medium sand. Sets of normal and reverse grading (from top to bottom) were also observed (**Figure 6**). Notably, the mean grain sizes of the candidate storm sediments of core 2 began to decrease slightly when compared with core 1 that contained very fine to fine sand (**Figure 6**). The mean grain size of core 3 was primarily fine to very fine sand and a pebble was also observed. The vertical variation in this core tended to show both fining and coarsening upwards (top to bottom) (**Figure 7**). Candidate storm sediments of core 4 contained only very fine sand, where the uppermost sample was characterized as coarse silt. Based on mean grain sizes, the deposits of candidate storm sediments found in this transect clearly show a landwards-fining trend.

Sorting

The sorting values of the beach sediments ranged between 0.62 and 1.02 phi scale, indicating moderately to moderately well sorted, except for recent beach 1 that was collected close to the present sea level and



showed a poorly sorted nature. Sorting values of candidate storm sediments ranged between 1.94 and 0.42 phi scale, showing a poorly, moderately, moderately well, and well-sorted nature. However, only three samples of the candidate storm sediments contained a well sorted sediment (core 2 at 236–238 cm depth). The vertical variations in the sorting values were also similar to the mean size (Figures 4, 6, 7). In other words, there were fluctuations in the sorting in the four ranges of core 1. Vertical changes in the sorting values from moderately to poorly sorted sand in core 1 were observed at a depth of 15–22, 23–29, 29.5–33, and 33.5–36 cm (Figure 4). Sorting values of core 2 showed three vertically opposite patterns (top to bottom) from poorly to moderately sorted at a depth of 9–15, 16–46, and 47–55 cm (Figure 6). Sorting values of the candidate storm sediments of core 3 displayed a poorly to moderately sorted nature, whereas sorting from top to bottom of core 4 were poorly to moderately sorted.

Skewness

Skewness indicates the asymmetry of a given frequency distribution. The positive value of skewness indicates coarse

dominated element, while negative value of skewness is fine (Folk and Ward, 1957). The skewness values of the beach sediment samples from the study area ranged between -0.74 and 0.02 phi scale. The recent beaches 1, 2 and ridge sediment 3 were classified as coarse skewed, while ridge sediments 1 and 2 were classified as symmetrical in nature. The skewness of the candidate storm sediment samples was apparent in the ranges of a very fine-skewed, fine-skewed, symmetrical, coarse-skewed and very coarse-skewed nature that ranged between -3.76 and 1.11 phi scale. However, the skewness values associated with the candidate storm sediments in each core were relatively complicated (Figures 4, 6, 7). For example, most of the skewness values of the candidate storm sediments of core 1 tended to be coarse-skewed, where other samples were shown as symmetrical, fine skewed, and very coarse-skewed (Figure 4). The main skewness values of the candidate storm sediments of core 2 were symmetrical. Subsequently, the minor values were present as fine skewed and coarse skewed, with only a few samples showing values in the very coarse skewed nature (Figure 6). Variation in the skewness values were also found in the candidate

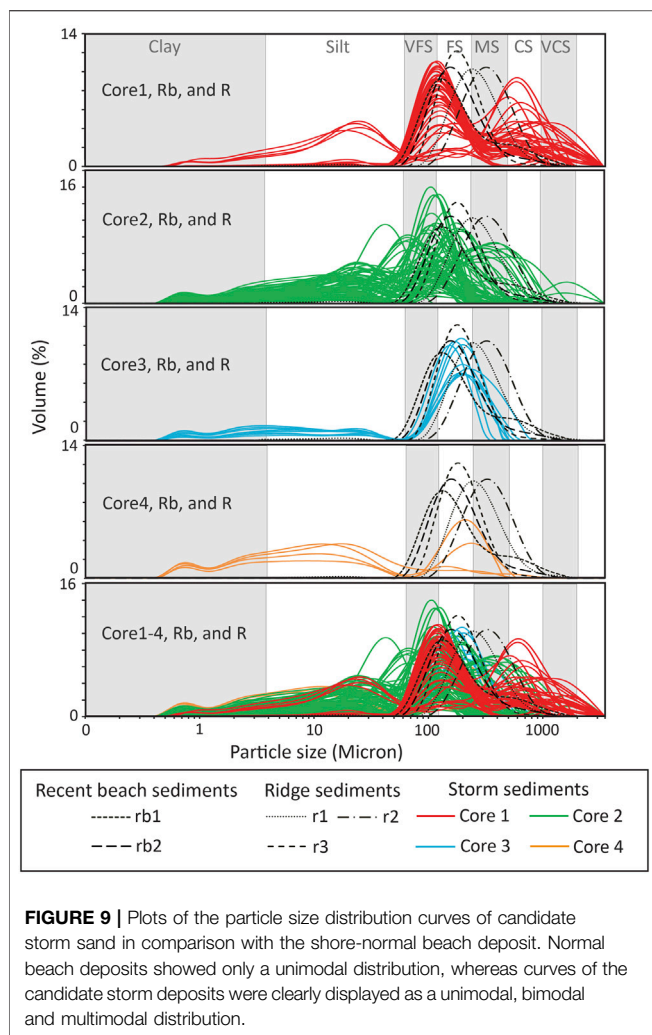


FIGURE 9 | Plots of the particle size distribution curves of candidate storm sand in comparison with the shore-normal beach deposit. Normal beach deposits showed only a unimodal distribution, whereas curves of the candidate storm deposits were clearly displayed as a unimodal, bimodal and multimodal distribution.

storm sediments of core 3, which consisted of symmetrical sediments at 15–23 cm depth, while fine-skewed sediments were found at 26–32 cm depth (Figure 7). The skewness values of the candidate storm sediments of core 4 showed coarse skewed and very coarse-skewed nature.

Kurtosis

Kurtosis is used to measure the degree of concentration of the grains relative to the average (Blott and Pye, 2001). The kurtosis values are similarly a function of the standard deviation; high kurtosis values are more apt to occur in well-sorted distributions, and low kurtosis values are more apt to occur in poorly sorted distribution (Cadigan, 1961). The low value of kurtosis displays the flattened shape of the curve (platykurtic), while the high value exhibits normal (mesokurtic) to very highly peaked shape (leptokurtic). The kurtosis values of the candidate storm and beach sediments, presented the different nature of distribution. Kurtosis values of candidate storm fell under a very platykurtic, platykurtic, mesokurtic, leptokurtic, and very leptokurtic nature of distribution, ranging between 1.44 and 12.33 phi scale. However, the beach sediments displayed kurtosis values

ranging in between 2.42 and 3.94 phi scale which fell under a platykurtic to early leptokurtic nature.

Grain Size Distribution

The grain size distribution curves of both the candidate storm and beach sediments were plotted and compared (Figure 9). The beach sediment curves showed only a unimodal distribution, falling under the range of fine and medium sand. In contrast, the candidate storm distribution curves showed three types of characteristics: unimodal, bimodal and multimodal distributions that fell under all ranges of sediment sizes, varying from clay to pebble in content. Based on the grain size distribution curves (Figure 9), the candidate storm sediments were similar to beach sediments and mostly fell under the sand-sized modes.

Age Determination of the Candidate Storm Deposits

Results of the OSL age determination obtained from the two beach ridges are shown in Table 1. The OSL dating results suggested the age of the inner beach ridge was $3,650 \pm 140$ to $3,034 \pm 106$ years ago (samples K5 and K4, respectively), while the ages of the outer beach ridge were in the period of $2,090 \pm 70$ to $1,160 \pm 30$ years ago (samples K2 and K1, respectively). Additionally, two cross-checking ages of the inner and outer beach ridge (samples K6 and K3, respectively) had ages of $3,034 \pm 106$ and $1,220 \pm 40$ years ago, respectively. We can infer that the age of the beach ridge plain in the southwestern part of the study area was older than in the northeastern part, with an age gap (hiatus) between the beach ridges of around 1,000 years ago. The four OSL ages derived from the latter part of the outer beach ridge (samples K7–10) indicated its formation during the late Holocene, giving ages from the top to bottom of $1,200 \pm 30$, $2,100 \pm 140$, $2,520 \pm 230$, and $2,650 \pm 350$ years ago at a depth of 20, 50, 65, and 85 cm, respectively. It is noted that the age of the two candidate storm layers at 50–58 and 65–72 cm depth was $2,100 \pm 140$ and $2,520 \pm 230$ years ago, respectively.

DISCUSSION

Sedimentary Diagnostic Key for Identifying Storm Deposits

The ancient washover deposits from the storm surge in this study area were interpreted based on the evidence found in both the surface and subsurface stratigraphy. Coastal swales, in general, have tied up calm water (low energy condition) such that fine particles brought in during heavy rain fall and/or high tide often progressively settle down in a suspension pattern. The presence of fine particles, such as clay and/or mud sizes is, therefore, regarded as the common sedimentation in the swale located at the southern part of this study area (Williams et al., 2016).

However, the stratigraphical evidences found in cores of this study at the Kui Buri swale, particularly the sand layers with sharp lower and upper contacts, were considered as the key feature of

storm events. Sedimentary structures, including parallel and inclined lamination, mud rip-up clast, layers of marine shell fragment, and sharp lower and upper contacts, indicated clearly the unusual process generated from a high energy event and transported sediments of each coastal zone into the swale environment.

Similar laminated structures of sand layers were observed at the southern part of Kui Buri, which indicated the interaction between the flow regimes and bottom current of the storm surge waves (Phantuwongraj et al., 2008). The laminated sand observed in this area reflected that the wave energy must have been strong enough to overtop the beach ridge and flow into the swale. The mud rip-up clasts found in core 2 in this area indicated that an eroded mud surface was torn up by the strong wave process and then laid down as a layer at the same time of deposition (e.g., Williams, 2013). Fragments of marine organisms (shells) were observed within the sand layers which have sharp lower and upper contacts with mud layers of swale. This is relatively clear that the sand layers found in stratigraphy were transported landwards from a marine origin.

Traces of abandoned channels remained observable in the western part of the study area, where Kui Buri River is located. However, these sedimentary structures found in the sand sheets were impossible to have been formed by fluvial transportation. Although flowing from flooding in the past can erode sand sediment from older landward beach ridges and redeposited in this swale, but it is refuted with the composition of the sediment we microscopically detected. The candidate storm sediment is backed up with the existence of marine microfossil while beach ridge sediment has no microfossil concentration. This is because marine organisms, such as calcareous foraminifera, ostracods and scaphopods, and marine shell fragments were found in every candidate storm layer. Most of the species of foraminifers found belonged to *Quinqueloculina* spp., *Spiroculina* spp., *Elphidium* sp., *Asterorotalia* sp., *Trochammina* sp. and *Ammonium* sp., which have various specific marine habitats, living on the sand surface of the open sea (shallow water), and are commonly found along the GOT (Jumnongthai, 1983; Melis and Violanti, 2006). Most importantly, it is almost impossible that the fossils of scaphopods (tusk shell), which commonly live in the mud or sand surface of the sea using their feet to burrow, would be in the harsh condition of this swale. The adaptation of some marine fauna may tolerate the very low salinity from increasing rain water, but in the summer, the swale will become dry. Thus, the swale was not the actual habitat for these marine microfauna. In any case, the swale water may be of a brackish nature because in periods of sea level maxima the sea water might be moved landwards through a channel where its boundary connected with the GOT. However, the dominant sedimentary structure (i.e., sharp contact) is too abrupt to be formed by the gradual movement landwards or seawards from the sea level rise.

Slope wash, or mass wasting process, in this area can be ruled out because the elevation of the topography at this site is not high enough to move sand-sized materials landwards and to form sand layers in the swale during heavy rainfall. Although, the instability of the beach ridge formation can move landwards to form a sand layer, the composition of the sand looks different. That is, the

composition of the beach ridge sand was at least 99% quartz, especially at the outer beach ridge (ridge sediment 3), but the sand composition in the swale had a relatively high concentration of bioclast content. This indicates that slope wash or mass wasting process in this area is highly unlikely.

Prehistorical and historical tsunami events deposited in this area can also be ruled out since no prehistorical and historical records of tsunami deposits have been recognized so far in the GOT. Only the Andaman coast of Thailand experienced devastating tsunami events, both recent (2004 Indian Ocean tsunami) and prehistoric (Jankaew et al., 2008). However, some researchers have pointed out that the possibility of a future tsunami in the GOT from a submarine tsunamigenic earthquake in the South-China Sea where the subduction zone is located. The nearest tectonic subduction zone close to the GOT is located at the Manila Trench at approximately 2,500 km. A magnitude Mw 9.0 submarine earthquake from the Manila Trench (Ruangrassamee and Saelem, 2009) would provide a maximum wave height of around 0.65 m directed toward the GOT coast.

Distinguishing Storm From Shore-normal Sediments

The common question on how to distinguish storm deposits from shore-normal sediments has always arisen among geoscientists. The simple answer taken here is that storm deposits are always overlain on beach sand and so they form as sand over sand layers. Although, they have similar sand features, they definitely are formed by different processes. Therefore, the way to distinguish storm from shore-normal sediments, especially from a beach ridge plain like in this study area, is challenging. Comparison between the grain size distribution curves of candidate storm and shore-normal beach sediments was performed (Figure 9) from which we suggest that they can be partly separated by the presence of various modal distributions that vary in the grain size of sediments in each coastal environmental zone and the depositional mechanism.

Frequency distribution curves of the beach sediments fall under fine and medium sand. In contrast, in many candidate storm sands the distribution curves exhibit a complex mixture of multiple modes, which means that the sediments were transported from mixtures of various sediment sources. Notably, the modes of some candidate storm distributions also fell under the range of clay, silt and pebble (Figure 9). The concordance of each mode reflects the correspondence of various sizes. Similar grain size distributions of both candidate storm and beach sediment distributions may indicate the environmental zone shown in the frequency curve associated with the transportation of a wave run-up. This suggests that beach sediments were swept into the swale by high energy waves of a coastal storm in the past.

Based on stratigraphy, all the candidate storm layers were discriminated by the presence of sedimentary structures, such as parallel and inclined landward lamination, mud rip-up clasts, marine shell fragment layer, and sharp lower and upper contacts. These structures were analyzed along with the data derived from the grain size analysis of candidate storm sediments and revealed

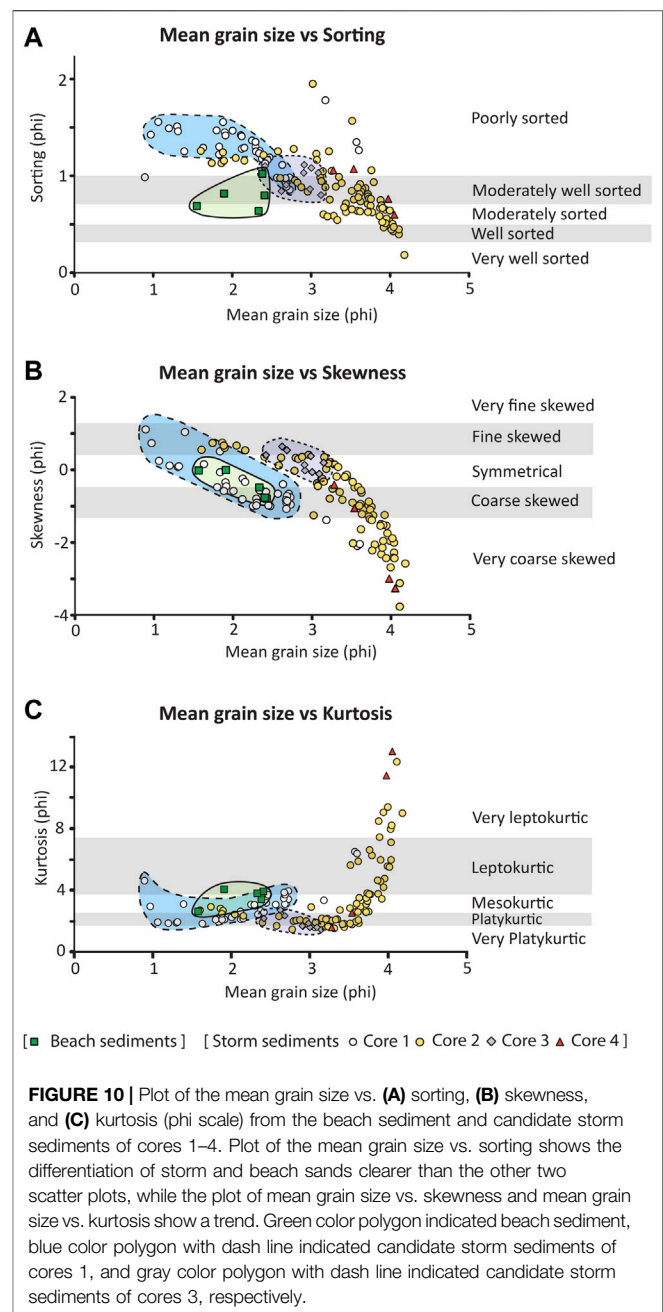
the impact of each flow and inundation regime of the coastal storm wave. In the initial stage, multiple wave sets of storm surges progressively increased by the strong wind speed of the coastal storm (swash regime) (Sallenger, 2000; Morton and Sallenger, 2003; Masselink and Heteren, 2014). Later, they overtopped on the beach ridge and transported an amount of eroded sediment landwards into the swale. During this stage, the inundation regime (Sallenger, 2000), which resulted from the increased surge velocity and surge height, lead to the sedimentary structures of the shell fragment layer (Figure 5F), laminated sand (Figures 5A,E), mud rip-up clast (Figure 5D), and multiple set of reverse and normal grading (Figures 4, 6, 7). This multiple grading reflected the hydrodynamic regimes during the inundation of the storm surge which were associated with the flow depth and indicated the upper flow regime conditions of a unidirectional, turbulent and high velocity flow (Cheel, 1990; Fielding, 2006).

In this process, grain size frequency distribution curves of the candidate storm sediments showed different modes compared to the curves of each coastal environmental zone of the shore-normal beach sediments (Figure 9). Moreover, the mean grain sizes of cores 1–4 point out that the coarser and heavier sand grains settled down first at the location in the processes of rolling, sliding, and saltation (cores 1–3), where the most seaward side forms the thickest sand layer (e.g., Liu, 2007).

While the influx of lighter sand grains along with the surge current was deposited as a suspension (Core 4), thinner and finer landward deposits (wedge shape) were formed (Figure 3B). In the latter stage, the lower flow regime condition resulting from the decreased surge energy led to a lamina flow condition and formed an unstructured candidate storm layer, as observed in the mean grain size variation in the candidate storm sediments of core 1 (Figure 4).

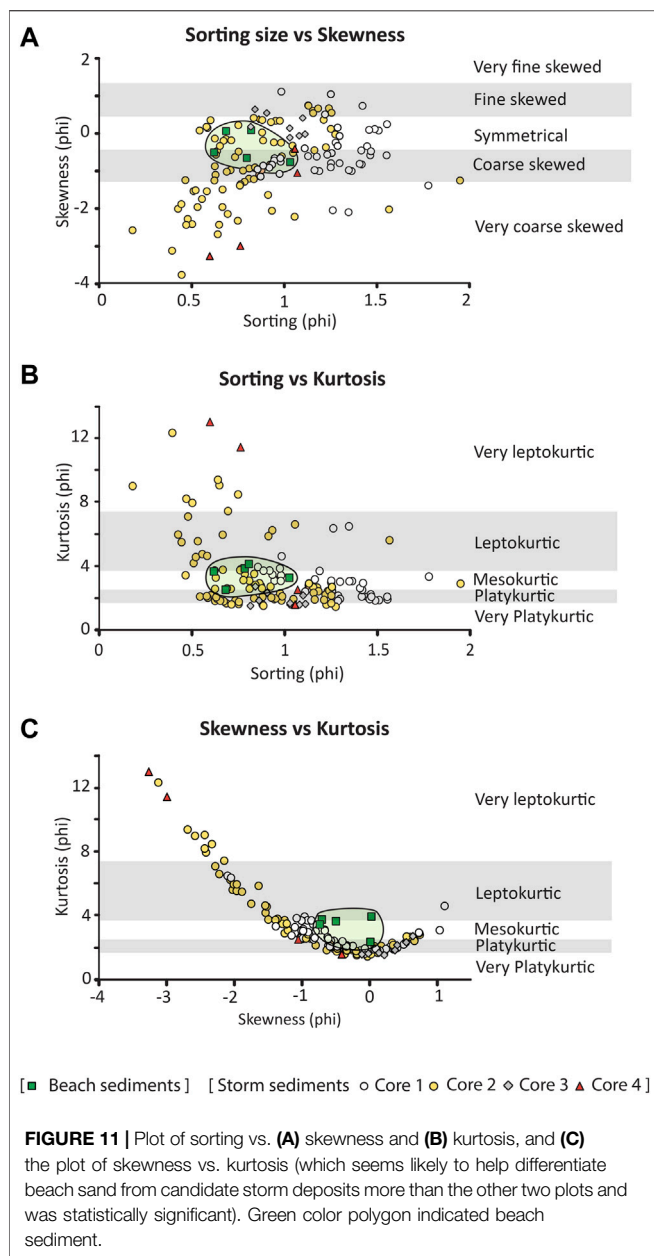
However, based on the grain size distribution curves of the shore-normal beach and candidate storm sediments (Figure 9), the difficulty to elucidate the source of candidate storm sediments in the range of very fine sand to silt in this study was evident. The possibility that the source of candidate storm sediments are from the swale itself and nearby creek or river channels by terrestrial flood can be ruled out based on the evidence of marine microfossil found in candidate storm deposits, while it does not appear in swale or creek sediments. Several finer sizes of storm sediments present in the comparative graphs have been transported from offshore during an extreme coastal storm. Wind speed and a high wave energy generated from an extreme coastal storm could stir up the entire water column with resuspended fine particles (fine sand, very fine sand, silt and mud) from the sea bottom surface where its depth was not too deep (Shanmugam, 2008).

In addition, the absence of finer sand at the recent beach was considered as a normal circumstance because the surf zone and/or breaker zone had significant impacts on the recent beach. Some of fine-grained particles were subjected to oscillatory water movement, where they were carried seawards by those waves from the breaker zone (Bagnold, 1963; Ingle, 1966) when the beach was adjoined to the open-sea. The sediment grains smaller than 0.150 mm (>2.75 phi) would be dispersed evenly within the water column and be carried offshore in a continual suspension. Additionally, grains smaller than 0.150 mm (>2.75 phi) are commonly absent from beach sand along open coasts, as the majority of grains smaller



than 0.140 mm are probably in suspension under all wave conditions (Friedman, 1967). However, the presence of major modes of candidate storm sediments ranging from clay, silt and pebble was not associated with the beach sediments, which suggested that the depositional process of a coastal storm event in the past remobilized the pre-existing sediments of each coastal zone landwards by storm surges.

An ability to differentiate the environmental zone between the river, beach, dune, and berm was made by plotting the statistical parameters derived from grain size analysis, including the mean grain size against sorting, skewness and kurtosis (e.g., Folk and Ward, 1957; Mason and Folk, 1958; Friedman, 1961). These plots are very beneficial because the



source of sands that belong to various environments have significantly different natural dynamic processes (Friedman, 1967). An attempt was made in this paper to differentiate storm and beach sediments (Figures 10, 11). The clearest and nearly complete separation group between candidate storm and shore-normal beach was the plot of the mean grain size against sorting (Figure 10A).

The statistical trends of plotting the candidate storm sediments were evaluated by plotting the mean grain size against the skewness and kurtosis and the skewness against kurtosis (Figures 10B,C,11C). The plot of mean grain size against skewness showed a significant trend of direct variation, where the more the mean grain size decreased, the more the skewness value decreased (Figure 10B). On the other hand, the plots of the mean grain size against kurtosis and that of skewness

against kurtosis show a reverse variation where the more the mean grain size decreased, the more the kurtosis values increased (Figure 10C), and the more the skewness value decreased, the more the kurtosis value increased (Figure 11C). The mean grain size, skewness and kurtosis values of the candidate storm sediments tended to be clearly associated with each other.

Age of the Ancient Storm Deposits and the Beach Ridges

The OSL dating results derived from the two beach ridges in the study area were used as an age control and also to help explain the evolution of the beach ridge formation in the past. Based on the OSL dating results, the inner beach ridge formed $3,650 \pm 140$ to $3,034 \pm 106$ years ago, while the outer beach ridge was formed $2,090 \pm 70$ to $1,160 \pm 30$ years ago. It is possible that the swale was formed about $2,090 \pm 70$ years ago after the outer beach ridge started accumulating. These ages for the beach ridges are consistent with the marine regression period, where a series of beach ridges prograded seawards as a result of the gradual decrease in sea level (Choowong et al., 2004).

The four OSL datings in the vertical depth of the outer beach ridge (trench) at 20, 50, 65, and 85 cm depth gave ages of $1,220 \pm 30$, $2,100 \pm 140$, $2,520 \pm 230$, and $2,650 \pm 350$ years ago, respectively. These ages are very important because, among the number of these four OSL ages, they consisted of two OSL ages of two candidate coastal storm events found at 50–58 cm and 65–72 cm depth ($2,100 \pm 140$ and $2,520 \pm 230$ years ago). Although, the depositional age of storm deposits at the deeper part (more than 85 cm depth) cannot be defined because there is no age-depth control in this study. However, we inferred from the results of the AMS dating of a nearby location (Williams et al., 2016) that it is 6,977 cal y B.P. at a depth 140 cm from the swale surface. If so, it can be concluded that the four extreme coastal storm events occurred in the periods of $2,100 \pm 30$ years ago to 6,977 cal y B.P. and the rest of the storm layers in the deeper part (20 layers) must be older than 6,977 cal y B.P.

As mentioned earlier in the part of geological setting, the ages of OSL dating resulted from our work can be related to the deposition of candidate storm sand layers during the period of progradation. Multiple candidate storm layers recognized from cores confirmed that the swale in this study area used to be a lagoon. Basically, a lagoon has a high preservation potential for the deposits of extreme coastal storms because the barrier beach sand itself is a major sediment source. Multiple layers of sand sheets intervened with pure mud are evidence to support their deposition in a lagoon environment.

CONCLUSION

In this study, records of ancient storm deposits were confirmed by sedimentological characteristics. The preservation of geological records of extreme storm events discovered along the coastal zone of the GOT suggests that the area is sensitive to such extreme storm events. Definitely, at Prachuap Khiri Khan southern peninsular Thailand, at least 21 layers of candidate coastal storm layers provide, as sedimentological evidence that

can be used as analogs for further research. These sedimentological analogs can be applied to areas that have similar geomorphological and geological conditions in this region.

Grain size distributions and statistical parameter plots were used to help differentiate candidate storm and shore-normal beach sediments in this study area. The plots of mean grain size against skewness and kurtosis and the plot of skewness against kurtosis show a trend. In conclusion, the shore normal-beach deposit was commonly described by a unimodal distribution, whereas candidate storm sediments appeared to have multimodal, bimodal and unimodal distributions, even in the same sand sheet.

The sedimentary structures of these storm deposits were similar to those that have been described in the literature. They include parallel and inclined landward laminations, mud rip-up clast, layer of shell fragments, pebble, normal and reverse gradings, sharp lower and upper contacts, and finer and thinner landward wedge-like shape deposits, plus the presence of marine microorganisms, including foraminifers, ostracods and scaphopods. These sedimentological characteristics described in this paper can be applied as a diagnostic key (locally valid indicator) or geological proxies of storm deposits in the region.

The OSL-based chronology and correlation with AMS age reported by Williams et al. (2016) provide the preservation potential of coastal storm frequency in the period of the middle to late Holocene. Linkage and application of this kind of paleotempestological research will increase our understanding of such hazards and be part of our responsibilities to mitigate the risk for coastal communities.

DATA AVAILABILITY STATEMENT

The original contributions presented in the study are included in the article/**Supplementary Material**, further inquiries can be directed to the corresponding author.

AUTHOR CONTRIBUTIONS

MC led the research. The study was designed and planned by all authors. SK and SP carried out fieldwork, sedimentological

analyses, and wrote the manuscript. OSL dating was performed by SK. Graphics and tables were made by SK and SP. MC involved essentially intellectual contributor, planned necessary fieldwork logistics, and funding acquisition. MC and SP provided critical discussions and contributions to the manuscript. All authors contributed to the article and approved the submitted version.

FUNDING

The 90th Anniversary Ratchadapisek Somphot Endowment Fund of Chulalongkorn University provided the fund to SK. SP was partially supported by Grants for Development of New Faculty Staff, Ratchadaphiseksomphot Endowment Fund, Chulalongkorn University (Grant no. GDNS 59-056-23-019). Climate Change and Disaster Management Cluster (CU59-060-CC) and Thailand Research Fund (BRG5780008) provided funds to MC and SP.

ACKNOWLEDGMENTS

MESA Research Unit of Department of Geology, Chulalongkorn University is acknowledged for logistic works and laboratory. The authors also thank to Preerasit Surakiatchai for fieldwork and OSL dating support. Finally, the authors would like to thank the editor and reviewers for providing constructive comments to improve the quality of this manuscript significantly.

SUPPLEMENTARY MATERIAL

The Supplementary Material for this article can be found online at: <https://www.frontiersin.org/articles/10.3389/feart.2021.625926/full#supplementary-material>.

Supplementary Table 1 | OSL Decay curve and Growth curve of each sample.

Supplementary Table 2 | Recycling ratio of each sample.

Supplementary Table 3 | Sediment composition, sphericity and roundness.

REFERENCES

- Bagnold, R. A. (1963). "Mechanics of marine sedimentation," in *The sea: ideas and observations on progress*. Editor M. L. Hill (New York, NY: Interscience), 3, 507–528.
- Bell, W. T. (1979). Attenuation factors for the absorbed radiation dose in quartz inclusion for thermoluminescence dating. *Ancient TL* 8, 2–13.
- Blott, S. J., and Pye, K. (2001). GRADISTAT: a grain size distribution and statistics package for the analysis of unconsolidated sediments. *Earth Surf. Process. Landforms* 26, 1237–1248. doi:10.1002/esp.261
- Bøtter-Jensen, L., Bulur, E., Duller, G. A. T., and Murray, A. S. (2000). Advances in luminescence instrument systems. *Radiat. Meas.* 32, 523–528. doi:10.1016/S1350-4487(97)00206-0
- Bøtter-Jensen, L. (1997). Luminescence techniques: instrumentation and methods. *Radiat. Meas.* 27, 749–768. doi:10.1016/S1350-4487(97)00206-0
- Cadigan, R. A. (1961). Geologic interpretation of grain-size distribution measurements of Colorado Plateau sedimentary rock. *J. Geol.* 69 (2), 121–144. doi:10.1086/626724
- Cheel, R. J. (1990). Horizontal lamination and the sequence of bed phases and stratification under upper-flow-regime conditions. *Sedimentology* 37, 517–529. doi:10.1111/j.1365-3091.1990.tb00151.x
- Chooiwong, M., Murakoshi, N., Hisada, K., Charusiri, P., Charoentitrat, T., Chutakositkanon, V., et al. (2008). Indian Ocean tsunami inflow and outflow at Phuket, Thailand. *Mar. Geol.* 248, 179–192. doi:10.1016/j.margeo.2007.10.011
- Chooiwong, M., Ugai, H., Charoentitrat, T., Charusiri, P., Daorerk, V., Songmuang, R., et al. (2004). Holocene biostratigraphical record in coastal deposits from Sam Roi Yod national park, Prachuap Khiri Khan, Western Thailand. *Nat. Hist. J. Chulalongkorn Univ.* 4, 1–18.
- Donnelly, J. P. (2005). Evidence of past intense tropical cyclones from back barrier salt pond sediment: a case study from Isla de Culebrita Puerto Rico, United States. *J. Coast Res.* 42, 201–210.

- Donnelly, J. P., Roll, S., Wengren, M., Butler, J., Lederer, R., and Webb, T., III (2001). Sedimentary evidence of intense hurricane strikes from New Jersey. *Geology* 29, 615–618. doi:10.1130/0091-7613(2001)029<0615:seoihs>2.0.co;2
- Duller, G. A. T. (2008). Single-grain optical of Quaternary sediments: why aliquot size matters in luminescence dating. *Boreas* 37, 589–612. doi:10.1111/j.1502-3885.2008.00051.x
- Elsner, J. B. (2007). Tempests in time. *Nature* 44, 647–649. doi:10.1038/447647a
- Fielding, C. R. (2006). Upper flow regime sheets, lenses, and scour fills: extending the range of architecture elements for fluvial sediment bodies. *Sediment. Geol.* 190, 227–240. doi:10.1016/j.sedgeo.2006.05.009
- Folk, R. L., and Ward, W. C. (1957). Brazos River bar: a study in the significance of grain size parameters. *J. Sediment. Petrol.* 27 (1), 3–26. doi:10.1306/74d70646-2b21-11d7-8648000102c1865d
- Friedman, G. M. (1961). Distinction between dune, beach, and river sands from their textural characteristics. *J. Sediment. Petrol.* 31, 514–529. doi:10.1306/74D70BCD-2B21-11D7-8648000102C1865D
- Friedman, G. M. (1967). Dynamic processes and statistical parameters compared for size frequency distributions. *J. Sediment. Petrol.* 37 (2), 327–354. doi:10.1306/74D716CC-2B21-11D7-8648000102C1865D
- Fritz, W. J., and Moore, J. N. (1988). *Basics of physical stratigraphy and sedimentology*. New York, NY: John Wiley, 371.
- Goff, J., McFadgen, B. G., and Chagué-Goff, C. (2004). Sedimentary differences between the 2002 easter storm and the 15th-century okoropunga tsunami, southeastern north island, New Zealand. *Mar. Geol.* 204, 235–250. doi:10.1016/s0025-3227(03)00352-9
- Ingle, J. C., Jr (1966). *The movement of beach sand*. New York, NY: Elsevier, 220.
- Jagodziński, R., Sternal, B., Szczuciński, W., Chagué-Goff, C., and Sugawara, D. (2012). Heavy minerals in the 2011 Tohoku-oki tsunami deposits—insights into sediment sources and hydrodynamics. *Sediment. Geol.* 282, 57–64. doi:10.1016/j.sedgeo.2012.07.015
- Jankaew, K., Atwater, B. F., Sawai, Y., Choowong, M., Charoentitirat, T., and MartinPrendergast, M. E. A. (2008). Medieval forewarning of the 2004 Indian Ocean tsunami in Thailand. *Nature* 455, 1228–1231. doi:10.1038/nature07373
- Jumongthai, J. (1983). Recent smaller foraminifera from the Gulf of Thailand. *Geol. Soc. Thailand* 6, 39–53.
- Komatsubara, J., Fujiwara, O., Takada, K., Sawai, Y., Aung, T. T., and Kamataki, T. (2008). Historical tsunamis and storms recorded in a coastal wetland, Shizuoka Prefecture, along the Pacific Coast of Japan. *Sedimentology* 55, 1703–1716. doi:10.1111/j.1365-3091.2008.00964.x
- Kongsen, S., Phantuwoongraj, S., and Choowong, M. (2016). “Possible ancient tropical storm layers from Prachuap Khiri Khan coastal area, the Gulf of Thailand,” in *The 42nd congress on science and technology of Thailand (STT42)*. Bangkok, Thailand: STT, 807–812.
- Kortekaas, S., and Dawson, A. G. (2007). Distinguishing tsunami and storm deposits: an example from Martinhal, SW Portugal. *Sediment. Geol.* 200, 208–221. doi:10.1016/j.sedgeo.2007.01.004
- Krumbein, W. C., and Pettijohn, F. J. (1938). *Manual of sedimentary petrography*. New York, NY: Appleton-Century-Crofts, 528–529.
- Liu, K. B. (2007). “Paleotempestology,” in *Encyclopedia of quaternary science*. Editor S. Elias (Amsterdam, Netherlands: Elsevier), 1978–1986.
- Liu, K. B., and Fearn, M. L. (2000a). “Holocene history of catastrophic hurricane landfalls along the Gulf of Mexico coast reconstructed from coastal lake and marsh sediments,” in *Current stresses and potential vulnerabilities: implications of global change for the Gulf Coast Region of the United States*. Editors Z. H. Ning and K. K. Abdollahi (Baton Rouge, United States: Gulf Coast Regional Climate Change Council and Franklin Press), 38–47.
- Liu, K. B., and Fearn, M. L. (1993). Lake-sediment record of late Holocene hurricane activities from coastal Alabama. *Geology* 21, 793–796. doi:10.1006/gres.2000.2166
- Liu, K. B., and Fearn, M. L. (2000b). Reconstruction of prehistoric landfall frequencies of catastrophic hurricanes in northwestern Florida from lake sediment records. *Quat. Res.* 54, 238–245. doi:10.1006/gres.2000.2166
- Liu, K. B. (2004). “Paleotempestology: geographic solutions to hurricane hazard assessment and risk prediction,” in *World minds: geographical perspectives on 100 problems*. Editors D. Janelle, B. Warf, and K. Hansen (Dordrecht, Netherlands: Kluwer Academic Publisher), 443–448.
- Mason, C. C., and Folk, R. L. (1958). Differentiation of beach, dune, and aeolian flat environments by size analysis, Mustang Island, Texas. *J. Sediment. Petrol.* 28, 211–226. doi:10.1306/74D707B3-2B21-11D7-8648000102C1865D
- Masselink, G., and Heteren, S. (2014). Response of wave-dominated and mixed-energy barriers to storms. *Mar. Geol.* 352, 321–347. doi:10.1016/j.margeo.2013.11.004
- McBride, E. F. (1971). “Mathematical treatment of size distribution data,” in *Procedures in sedimentary petrology*. Editor R. F. Carver (New York, NY: Wiley Interscience), 109–127.
- Melis, R., and Violanti, D. (2006). Foraminiferal biodiversity and Holocene evolution of the Phetchaburi coastal area (Thailand gulf). *Mar. Micropaleontol.* 61, 94–115. doi:10.1016/j.marmicro.2006.05.006
- Morton, R. A., Gelfenbaum, G., and Jaffe, B. R. (2007). Physical criteria for distinguishing sandy tsunami and storm deposits using modern examples. *Sediment. Geol.* 200, 184–207. doi:10.1016/j.sedgeo.2007.01.003
- Morton, R. A., and Sallenger, A. H., Jr (2003). Morphological impacts of extreme storms on sandy beaches and barriers. *J. Coast Res.* 19, 569–573.
- Murray, A. S., Marten, R., Johnson, A., and Martin, P. (1987). Analysis for naturally occurring radionuclides at environment concentrations by gamma spectrometry. *J. Radioanal. Nucl. Chem.* 115, 263–288. doi:10.1007/bf02037443
- Murray, A. S., and Wintle, A. G. (2000). Luminescence dating of quartz using an improved single-aliquot regenerative-dose protocol. *Radiat. Meas.* 32, 57–73. doi:10.1016/s1350-4487(99)00253-x
- Nanayama, F., Shigeno, K., Satake, K., Shimokawa, K., Koitabashi, S., Miyasaka, S., et al. (2000). Sedimentary differences between the 1993 Hokkaido-nansei-oki tsunami and the 1959 Miyakojima typhoon at Taisei, southwestern Hokkaido, northern Japan. *Sediment. Geol.* 135, 255–264. doi:10.1016/s0037-0738(00)00076-2
- Nott, J. (2007). The importance of Quaternary records in reducing risk from tropical cyclones. *Paleogeograph. Paleoclimatol. Paleocol.* 251, 137–149. doi:10.1016/j.palaeo.2007.02.024
- Phantuwoongraj, S., Choowong, M., and Chutakositkanon, V. (2008). “Possible storm deposits from Surat Thani and Nakhon Si Thammarat provinces, the southern peninsular Thailand.” in Proceedings of the international symposium on geoscience resources and environments of asian terranes, Bangkok, Thailand, November 19–20, 2008 (Bangkok, Thailand: GREAT), 395–399.
- Phantuwoongraj, S., Choowong, M., Nanayama, F., Hisada, K., Charusiri, P., Chutakositkanon, V., et al. (2013). Coastal geomorphic conditions and styles of storm surge washer deposits from Southern Thailand. *Geomorphology* 192, 43–58. doi:10.1016/j.geomorph.2013.03.016
- Phantuwoongraj, S., Choowong, M., and Silapanth, P. (2010). Geological evidence of sea-level change: a preliminary investigation at Panang Tak area, Chumphon province, Thailand. The 117th annual meeting of the geological society of Japan, March 31, 2011 (Chiyoda, Tokyo: The Geological Society of Japan), 369, 24.
- Phantuwoongraj, S., and Choowong, M. (2012). Tsunami versus storm deposits from Thailand. *Nat. Hazards* 63, 31–50. doi:10.1007/s11069-011-9717-8
- Powers, M. C. (1953). A new roundness scale for sedimentary particle. *J. Sediment.* 23, 117–119. doi:10.1306/D4269567-2B26-11D7-8648000102C1865D
- Prescott, J. R., and Hutton, J. T. (1994). Cosmic ray distributions to dose rates for luminescence and ESR dating: large depths and long-term variations. *Radiat. Meas.* 23, 497–500. doi:10.1016/1350-4487(94)90086-8
- Rosenthal, Y., Holbourn, A. E., Kulhanek, D. K., Aiello, I. W., Babila, T. L., Bayon, G., et al. (2018). “Expedition 363 methods,” in Proceedings of the international ocean discovery program, 363, College Station, TX, June 8, 2018 (International Ocean Discovery Program), 102.
- Rothwell, R. G. (1989). *Minerals and mineraloids in marine sediments: an optical identification guide*. London, United Kingdom: Elsevier, 279.
- Roy, P. S. (1990). UNESCO Mission report. Offshore minerals exploration in the Gulf of Thailand: review of quaternary geology of the coast an offshore seabed in exploration area 2. Available at: <https://whc.unesco.org/en/documents/> (Accessed February 4–28, 1990).
- Ruangrassamee, A., and Saelem, N. (2009). Effect of tsunami generated in the Manila Trench on the Gulf of Thailand. *J. Asian Earth Sci.* 36, 56–66. doi:10.1016/j.jseae.2008.12.004
- Sallenger, J. A. H. (2000). Storm impact scale for barrier island. *J. Coast Res.* 16, 890–895.
- Shanmugam, G. (2008). The constructive functions of tropical cyclones and tsunamis on deep-water sand deposition during sea water high stand: implications for petroleum exploration. *AAPG (Am. Assoc. Pet. Geol.) Bull.* 92, 443–471. doi:10.1306/12270707101

- Surakiatchai, P., Choowong, M., Charusiri, P., Charoentitirat, T., Chawchai, S., Pailoplee, S., et al. (2018). Middle to late Holocene paleogeography and history of sea level change from Sam Roi Yot national Park, Gulf of Thailand. *Trop. Nat. Hist.* 18 (2), 112–134.
- Tuttle, M., Raffman, A., Anderson, T., and Jeter, H. (2004). Distinguishing tsunami from storm deposits in North America: the 1929 grand banks tsunami versus the 1991 halloween storm. *Seismol Res. Lett.* 15, 117–131. doi:10.1785/gssrl.75.1.117
- Vongvisessomjai, S. (2009). Tropical cyclone disasters in the Gulf of Thailand. *Songklanakarin J. Sci. Technol.* 31 (2), 213–227.
- Williams, H. F. L. (2013). 600 year sedimentary archive of hurricane strikes in a prograding beach ridge plain, southwestern Louisiana. *Mar. Geol.* 336, 170–183. doi:10.1016/j.margeo.2012.12.005
- Williams, H. F. L., Choowong, M., Phantuwongraj, S., Surakietchai, P., Kongsen, S., and Simon, E. (2016). Geologic records of Holocene typhoon strikes on the Gulf of Thailand coast. *Mar. Geol.* 372, 66–78. doi:10.1016/j.margeo.2015.12.014
- Williams, H. F. L. (2010). Storm surge deposition by hurricane ike on the McFadden national wildlife refuge, Texas: implication for paleotempestology studies. *J. Foraminifer. Res.* 40, 210–219. doi:10.2113/gsjfr.40.3.210

Conflict of Interest: The authors declare that the research was conducted in the absence of any commercial or financial relationships that could be construed as a potential conflict of interest.

Copyright © 2021 Kongsen, Phantuwongraj and Choowong. This is an open-access article distributed under the terms of the Creative Commons Attribution License (CC BY). The use, distribution or reproduction in other forums is permitted, provided the original author(s) and the copyright owner(s) are credited and that the original publication in this journal is cited, in accordance with accepted academic practice. No use, distribution or reproduction is permitted which does not comply with these terms.